Journal of Translational Medicine

RESEARCH

Open Access

YY1-induced DDX18 modulates EMT via the AKT/mTOR pathway in esophageal cancer: a novel therapeutic target

Xiaochao Ma[1], Yulu He[2], Yue Yang[1], Tianyu Lu[1], Ze Tang[1], Youbin Cui[1*] and Rui Wang[1*]

Abstract

Background Esophageal cancer is the 11th most common malignancy and the 7th leading cause of cancer-related death globally. Identifying key molecules and underlying mechanisms in the progression of esophageal cancer represents an effective strategy for developing novel therapeutic approaches.

Methods *DDX18* expression in clinical specimens was evaluated by immunohistochemistry and western blot analysis. Functional assays were performed in cells with either *DDX18* knockdown or overexpression. Dual luciferase reporter assays and chromatin immunoprecipitation (ChIP) were conducted to validate the interaction between *YY1* and the *DDX18* promoter. A xenograft tumor model was utilized to investigate the role of *DDX18* in vivo in esophageal cancer.

Results *DDX18* was found to be markedly overexpressed in esophageal cancer, with its levels significantly higher in patients with pathological grade III compared to those with grades I–II. In vitro, *DDX18* enhanced cell proliferation, migration, and invasion, while concurrently suppressing apoptosis. Furthermore, *DDX18* promoted epithelial–mesenchymal transition (EMT) and activated the *AKT/mTOR* signaling pathway. The use of *AKT* inhibitors effectively abrogated the oncogenic effects of *DDX18*. Dual luciferase and ChIP assays confirmed that *YY1* binds to and stimulates *DDX18* transcription. In rescue experiments, *YY1* countered the inhibitory effects of *DDX18* knockdown on cell proliferation, EMT, and *AKT/mTOR* activation. In vivo, *DDX18* knockdown resulted in reduced tumor growth.

Conclusions The transcription of *DDX18* was activated by *YY1*, and *DDX18* promoted tumor cell growth and EMT through the *AKT/mTOR* signaling pathway in esophageal cancer cells.

Keywords *DDX18*, Esophageal cancer, Transcription factor, EMT, Apoptosis

*Correspondence:
Youbin Cui
cuiyb@jlu.edu.cn
Rui Wang
ruiwang14@mails.jlu.edu.cn
[1]Department of Thoracic Surgery, Organ Transplantation Center, The First Hospital of Jilin University, 1 Xinmin Street, Changchun, Jilin 130021, China
[2]Genetic Diagnosis Center, The First Hospital of Jilin University, Changchun, Jilin 130021, China

Introduction

Esophageal cancer ranks as the 11th most common cancer and stands as the 7th leading cause of cancer-related mortality worldwide [1]. Due to its insidious onset and the limitations of current diagnostic techniques, the efficacy of surgery, radiotherapy, and chemotherapy remains suboptimal [2]. Survival rates are dismal, with only 15–25% of patients surviving five years or more following diagnosis [3]. In contrast, molecular-targeted therapies have already transformed the management of several solid tumors, paving the way for more personalized and precise treatment strategies [4, 5]. Consequently, investigating pivotal molecules and their mechanisms in esophageal cancer progression may yield new therapeutic targets.

DEAD (*Asp-Glu-Ala-Asp*) *box polypeptide 18* (*DDX18*) belongs to the DEAD box protein family—a group of highly conserved RNA helicases [6, 7]. *DDX18* is implicated in various RNA modifications, including translation initiation, nuclear and mitochondrial splicing, and the assembly of ribosomes and spliceosomes [8, 9]. Aberrant expression of *DDX18* has been documented in gastric, breast, and pancreatic cancers, correlating with distinct tumor cell characteristics [10–12]. Notably, Chen et al. identified *DDX18* as a hub gene in esophageal cancer through GEO analysis, demonstrating its abnormal overexpression in patient tumor tissues [13]. These findings suggest that *DDX18* may play a crucial role in the pathogenesis of esophageal cancer, although its precise involvement has not been previously reported.

In this study, we investigated the functional effects of *DDX18* on esophageal cancer and explored the associated molecular mechanisms. Our findings offer novel insights into the progression of esophageal cancer and potential avenues for treatment.

Materials and methods

Samples

A total of 24 tumor specimens from esophageal cancer patients were collected from the First Hospital of Jilin University. In addition, a tissue array comprising 45 esophageal cancer and 45 adjacent non-tumor tissues was obtained from WeiaoBio (Shanghai, China). All experimental procedures were approved by the Institutional Review Board of the First Hospital of Jilin University.

Immunohistochemistry

Tissue arrays were deparaffinized, rehydrated, and subjected to antigen retrieval. After blocking with goat serum, arrays were incubated with a *DDX18* primary antibody at 4 °C overnight, followed by a secondary antibody at 37 °C for 30 min. DAB (Maxim, Fuzhou, China) was employed for visualization, and images were captured at 40× and 100× magnifications.

Cells

Human esophageal cancer cell lines (KYSE-150, TE1, KYSE450, KYSE140, and KYSE-30) were procured from the American Type Culture Collection (ATCC, Manassas, VA, USA). Cells were cultured in RPMI 1640 supplemented with 10% foetal bovine serum (FBS), 100 U/mL penicillin, and 100 mg/mL streptomycin. Transfections were performed with Lipofectamine 2000 (Invitrogen, Carlsbad, CA, USA) when cells reached over 85% confluence. KYSE-30 cells were treated with 10 μM *AKT* inhibitor LY294002 for 24 h in rescue experiments.

Real-time quantitative PCR (qPCR)

Post-transfection, cells were collected for RNA extraction using Trizol (Solarbio Science & Technology, Beijing, China). cDNA synthesis was carried out with the SuperRT cDNA Synthesis Kit (CWBio, Beijing, China), and qPCR was performed with MagicSYBR Mixture (CWBio, Beijing, China) according to the manufacturer's instructions. Gene expression was quantified using the $2^{-\Delta\Delta Ct}$ method, with *GAPDH* serving as an internal control.

Western blot

Following 24 h of transfection, cells were lysed with RIPA buffer. Proteins were separated by SDS-PAGE and transferred onto PVDF membranes (Millipore, Germany). After blocking with non-fat milk, membranes were incubated with primary antibodies for 1 h at room temperature, followed by secondary antibodies for another hour. Bands were visualized using an enhanced ECL kit, and densitometric analysis was performed with ImageJ software.

Cell-counting Kit-8 (CCK-8)

Cell viability was determined using the CCK-8 assay. Cells were seeded in 96-well plates at a density of 1×10^4 cells per well post-transfection. After adding 10 μL of CCK-8 reagent and incubating for 2 h at 37 °C, the optical density (OD) was measured at 450 nm.

Colony formation assay

Cells were plated in 12-well plates and incubated for 14 days. Colonies were fixed with 4% paraformaldehyde, stained with crystal violet for 15 min, and subsequently photographed and counted.

Transwell migration and invasion assays

For migration assays, 1×10^5 cells suspended in serum-free/serum medium were seeded into the upper chamber of Transwell inserts, with the lower chamber containing medium supplemented with 10% FBS. After 48 h of incubation, migrated cells were fixed with 4%

paraformaldehyde and stained with 0.5% crystal violet, then counted at 100× magnification.

Wound healing assay

Post-transfection, cells were seeded in 12-well plates and cultured at 37 °C for 24 h. Wounds were created using a micropipette tip, and images were captured at 40× magnification every 24 h. Wound closure was quantified using ImageJ.

Cell cycle detection

Cells were fixed in 70% ethanol 24 h post-transfection and stained with propidium iodide (PI) in the dark at room temperature for 30 min. Cell cycle distribution was analyzed by flow cytometry and evaluated with FlowJo software.

Cell apoptosis detection

Following transfection, cells were harvested and stained with Annexin V/FITC and PI (4 A BIOTECH, Beijing, China). Apoptotic cells were quantified using flow cytometry and analyzed with FlowJo software.

Dual luciferase assay

The binding site between *YIN-YANG 1* (*YY1*) and *DDX18* promoter was predicted using JASPAR (https://jaspar.elixir.no/) [14]. Wild-type or mutant binding sequences were cloned into the pGL3-Report luciferase vector. These constructs were co-transfected with a *YY1* overexpression plasmid into 293T cells, and luciferase activities (firefly and renilla) were measured using a dual-luciferase reporter system.

Chromatin Immunoprecipitation assay (CHIP)

The Magna ChIP™ Protein G Kit (Millipore, Cork, Ireland) was utilized to assess the interaction between *YY1* and the *DDX18* promoter in KYSE-150 and KYSE-30 cells. Following immunoprecipitation with an anti-*YY1* antibody, qPCR was performed to determine the enrichment of *DDX18*.

Establishment of animal model

Female BALB/C mice were subcutaneously injected with 1×10^6 KYSE-150 or TE-1 cells ($n = 5$ per group). After 24 days, mice were euthanized, and tumors were excised and measured. *DDX18* expression was further evaluated by immunohistochemistry.

Statistical analysis

Data are presented as mean ± SD from at least three independent experiments. One-way ANOVA was used for statistical comparisons between groups, with significance defined as $P < 0.05$.

Table 1 *DDX18* expression in EC compared with para-carcinoma tissue

Group	n	*DDX18* expression		*P*
		Low (n %)	High (n %)	
EC	45	17 (37.8)	28 (62.2)	0.001**
Para-carcinoma	45	33 (73.3)	12 (26.7)	

** $P < 0.01$

Table 2 *DDX18* expression associated with the clinicopathological parameters in esophageal cancer

Clinicopathological parameters	*n*	DDX18 Low (*n* %)	DDX18 High (*n* %)	*P*
Gender				
Male	41	16 (39.0)	25 (61.0)	0.990
Female	4	1 (25.0)	3 (75.0)	
Age (years)				
≤65	25	10 (40.0)	15 (60.0)	0.973
>65	20	7 (35.0)	13 (65.0)	
Pathological grading				
I-II	33	16 (48.5)	17 (51.5)	0.035*
III	12	1 (8.3)	11 (91.7)	

* $P < 0.05$

Results

DDX18 was upregulated in esophageal cancer

Analysis of a tissue array comprising 45 tumor and 45 para-carcinoma samples revealed that *DDX18* expression was significantly higher in tumor tissues (28 out of 45, 62.2%) compared to para-carcinoma tissues (12 out of 45, 26.7%) (Table 1). Notably, patients with pathological grade III tumors exhibited significantly higher *DDX18* expression than those with grades I–II (Table 2).

Further validation using 24 paired clinical specimens demonstrated elevated *DDX18* expression in tumor tissues by both qPCR and western blot (Fig. 1B and C). Among five esophageal cancer cell lines examined, KYSE-150 displayed the highest *DDX18* levels, whereas KYSE-30 exhibited the lowest, at both mRNA (Fig. 1D) and protein (Fig. 1E) levels; hence, these cell lines were selected for subsequent functional studies.

DDX18 promoted proliferation, migration, and invasion of esophageal cancer cells

To investigate the role of *DDX18* in regulating the behavior of esophageal cancer cells, we constructed an overexpression plasmid for *DDX18* and designed siRNAs to target its expression. In KYSE-150 cells, transfection with *DDX18* siRNAs led to a marked reduction in *DDX18* levels compared to cells treated with scrambled siRNA (Fig. 2A and B). Conversely, in KYSE-30 cells, transfection with the *DDX18* overexpression plasmid resulted in a significant increase in *DDX18* levels relative to the empty vector control (Fig. 2A and B). Cell proliferation was assessed using CCK8 and colony formation assays. The CCK8 assay revealed a notable decrease in optical

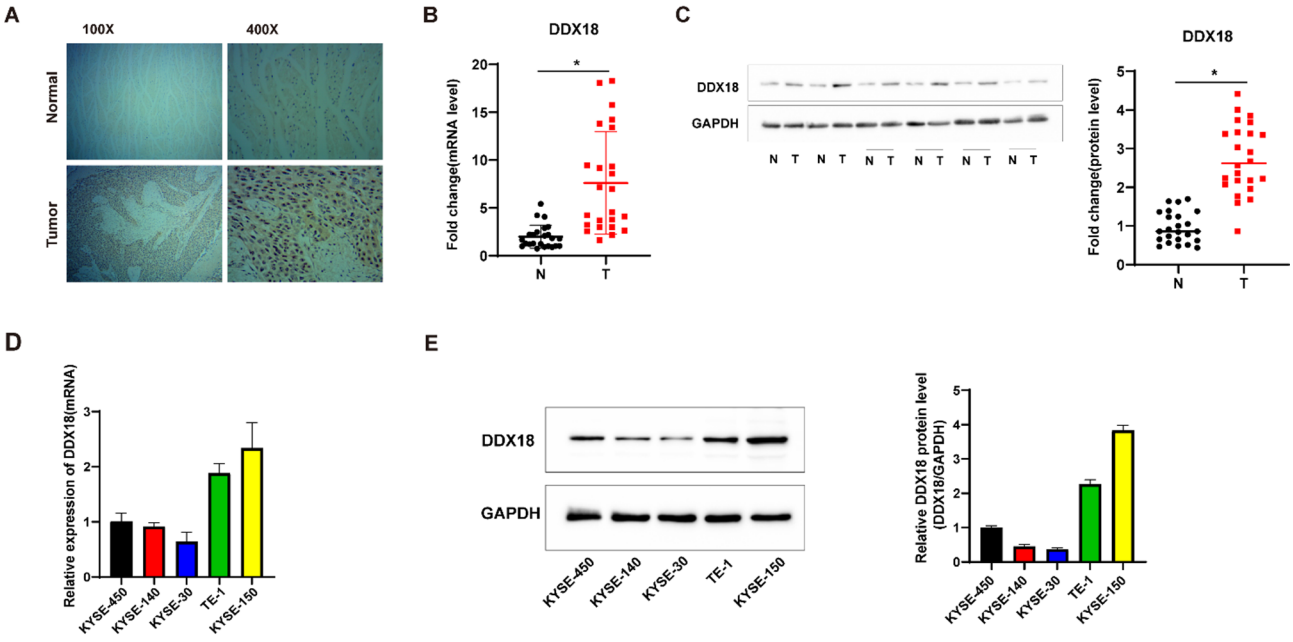

Fig. 1 *DDX18* was upregulated in esophageal cancer. (**A**) Immunohistochemical analysis of *DDX18* expression in a tissue array comprising 45 esophageal cancer tissues and 45 adjacent non-tumor tissues. (**B**) qPCR analysis of *DDX18* mRNA expression in 24 paired esophageal cancer and adjacent non-tumor tissues. (**C**) Western blot analysis of *DDX18* protein expression, with *GAPDH* as the loading control. (**D**) qPCR detection of *DDX18* mRNA levels in human esophageal cancer cell lines KYSE-150, TE-1, KYSE-450, KYSE-140, and KYSE-30. (**E**) Western blot analysis of *DDX18* protein expression in esophageal cancer cell lines, with *GAPDH* as the loading control. * $P < 0.05$

density values in *DDX18* knockdown cells compared to control cells (Fig. 2C); while *DDX18* overexpression led to a considerable increase (Fig. 2C). Similarly, colony formation results indicated that the number of colonies was significantly reduced upon *DDX18* silencing and markedly elevated following *DDX18* overexpression (Fig. 2D and E).

Subsequently, migration and invasion capabilities were evaluated using Transwell and wound healing assays. The Transwell assay demonstrated that *DDX18* siRNA substantially diminished the number of migrated and invasive cells in KYSE-150 cells (Fig. 2F), whereas *DDX18* overexpression enhanced these parameters in KYSE-30 cells (Fig. 2G). Consistently, wound healing assays showed that cells with *DDX18* knockdown had a significantly smaller wound closure area, while those with increased *DDX18* expression exhibited a larger healing area (Fig. 2H and I).

DDX18 increased the number of G2/M phase cells

After 24 h post-transfection, cell cycle analysis was performed in both KYSE-150 and KYSE-30 cells. In KYSE-150 cells, *DDX18* knockdown resulted in a noticeable increase in the percentage of cells in the G0/G1 phase and a marked decrease in those in the G2/M phase (Fig. 3A). Conversely, in KYSE-30 cells, overexpression of *DDX18* led to a significant reduction in G0/G1 phase cells alongside an increase in S and G2/M phase cells (Fig. 3B). To elucidate the underlying mechanism, we examined key cell cycle regulators (Fig. 3C). In KYSE-150 cells, *DDX18* knockdown suppressed the expression of *Cyclin D1*, *cMyc*, and *CDK4*, while in KYSE-30 cells, *DDX18* overexpression enhanced their levels (Fig. 3D). In contrast, the expression of *P21* was elevated in the *DDX18*-silenced cells and reduced in cells with *DDX18* overexpression (Fig. 3D).

DDX18 inhibited apoptosis in esophageal cancer cells

To thoroughly examine *DDX18*'s impact on cellular function, we assessed apoptosis by flow cytometry (Fig. 4A). In agreement with our previous findings, silencing *DDX18* led to an increase in apoptotic cells, while its overexpression resulted in a reduction (Fig. 4B). At the molecular level, *DDX18* knockdown caused a decrease in *BCL2* expression, whereas its overexpression elevated *BCL2* levels (Fig. 4C and D). In contrast, the levels of *BAX* and *active Caspase-3* were increased following *DDX18* silencing and decreased when *DDX18* was overexpressed (Fig. 4C and D). These data confirm that *DDX18* acts to suppress apoptosis in esophageal cancer cells.

DDX18 induced EMT in esophageal cancer cells

Subsequently, EMT-related proteins were assessed by western blot analysis. As illustrated in Fig. 4E and F, *DDX18* silencing led to an increase in the epithelial marker *E-cadherin*, whereas its overexpression resulted

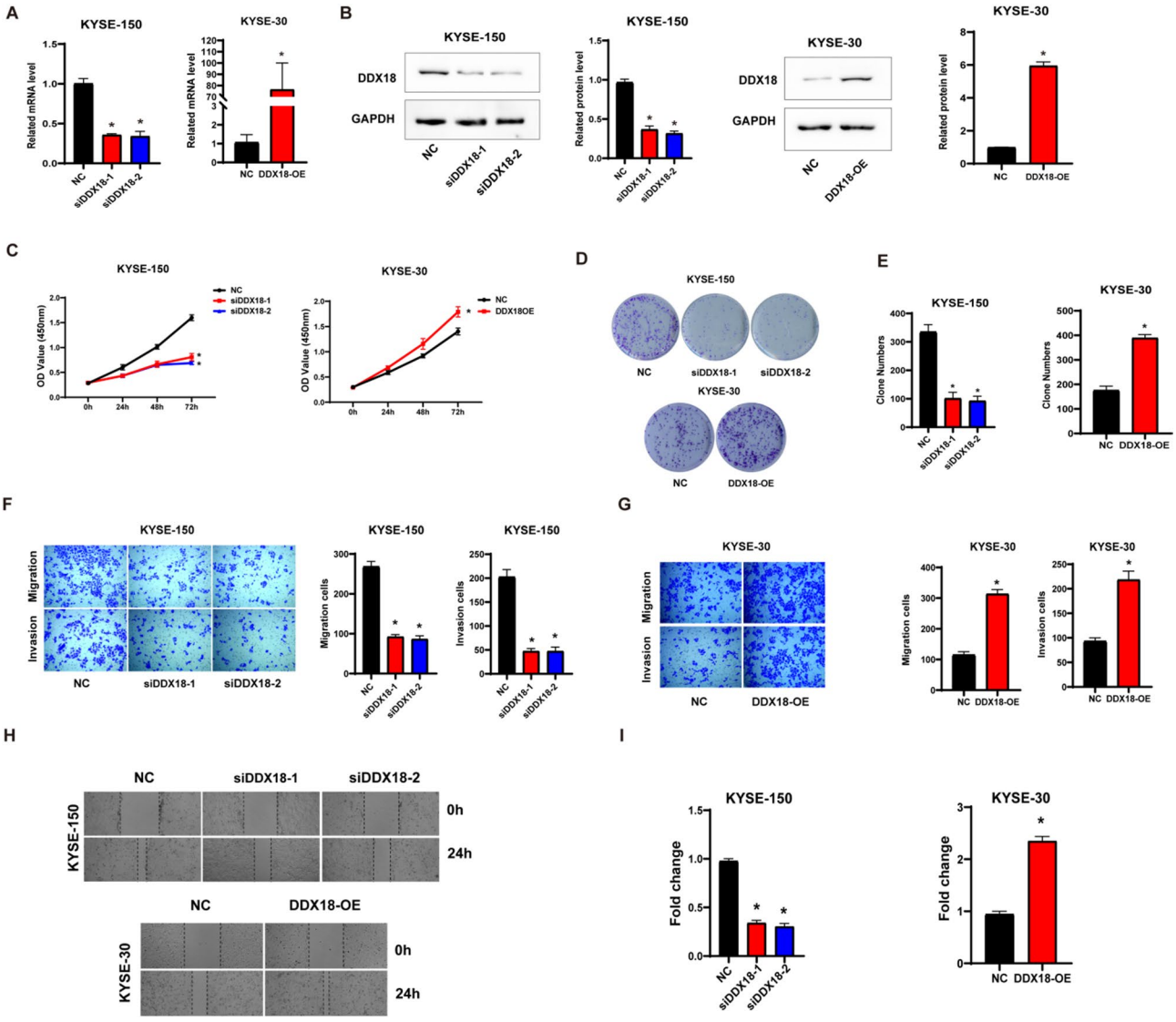

Fig. 2 *DDX18* promoted the proliferation, migration, and invasion in esophageal cancer cells. (**A**) KYSE-150 and KYSE-30 cells were transfected with *DDX18* siRNA and *DDX18* overexpression plasmid, respectively. qPCR was performed to assess *DDX18* expression levels. (**B**) Western blot analysis of *DDX18* protein expression. (**C**) Cell viability was evaluated using the CCK-8 assay. (**D**) Representative images from the colony formation assay, captured 14 days post-transfection. (**E**) Quantification of colony numbers in each group. (**F**, **G**) Transwell assays were conducted to assess the migration and invasion abilities of KYSE-150 (**F**) and KYSE-30 (**G**) cells. Images were captured at 100× magnification. (**H**) Wound healing assay images taken at 0 h and 24 h, captured at 40× magnification. (**I**) Quantification of wound healing areas, normalized to the control group. * $P < 0.05$

in decreased *E-cadherin* levels. Conversely, mesenchymal markers—including *N-cadherin*, *SLUG*, *SNAIL*, and *Vimentin*—were suppressed when *DDX18* was knocked down and elevated upon its overexpression. These findings suggest that *DDX18* facilitates EMT in esophageal cancer cells.

DDX18 activated the *AKT*/*mTOR* signaling pathway

We then examined the signaling pathway modulated by *DDX18* in esophageal cancer cells. Our data show that phosphorylation of *AKT* and *mTOR* was markedly reduced in cells with *DDX18* knockdown and significantly increased in cells overexpressing *DDX18* compared with controls (Fig. 4G and H). In addition, the expression levels of downstream effectors, including *P70/S6K*, *FOX*, and *Palladin*, were suppressed by *DDX18* silencing in KYSE-150 cells, whereas they were elevated in KYSE-30 cells following *DDX18* overexpression (Fig. 4G and H). These observations imply that *DDX18* enhances esophageal cancer progression by activating the *AKT*/*mTOR* signaling pathway.

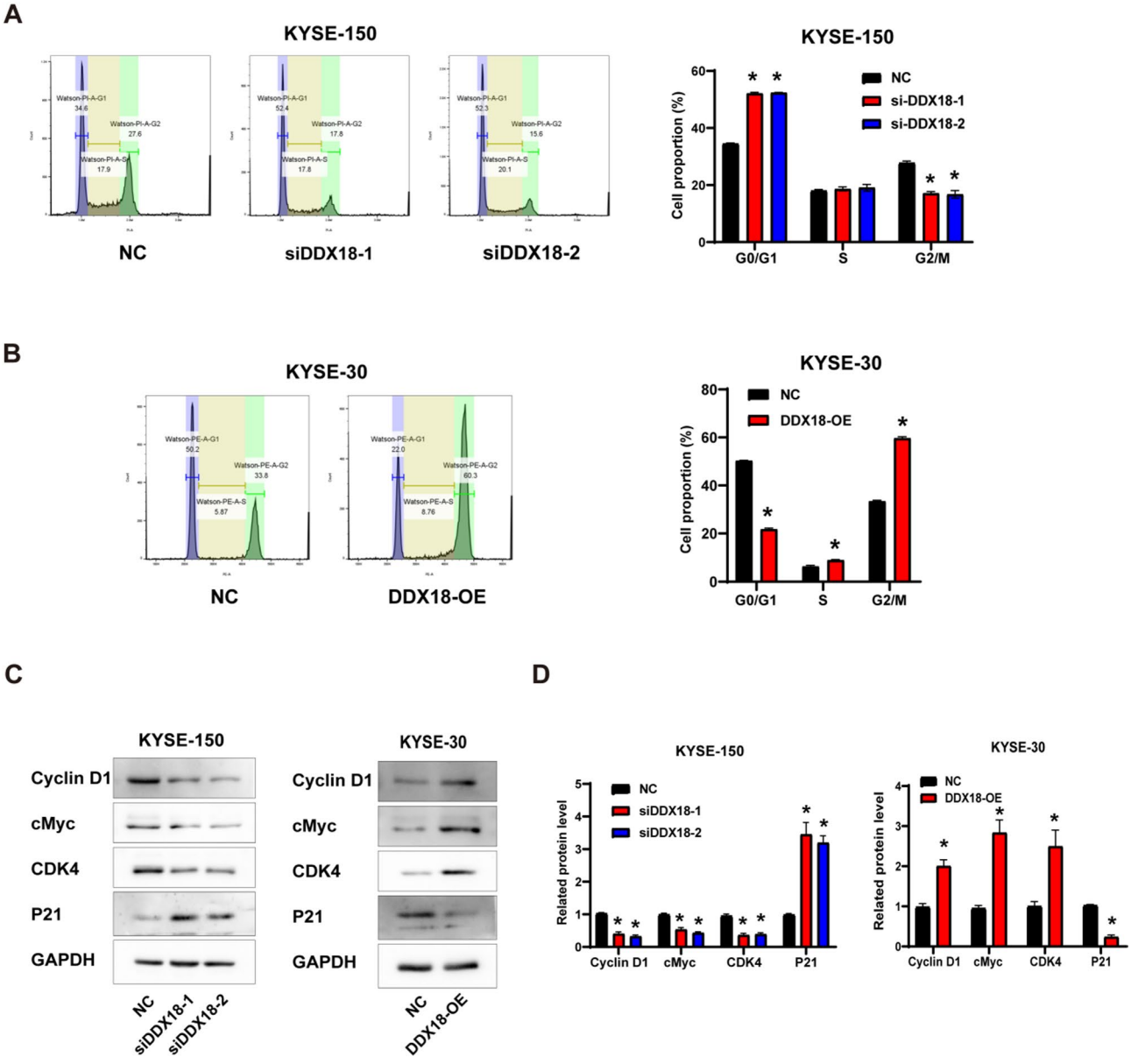

Fig. 3 *DDX18* increased the G2/M phase cells. (**A**, **B**) Cell cycle distribution (G0/G1, S, and G2/M phases) was analyzed in KYSE-150 (**A**) and TE-1 (**B**) cells 24 h post-transfection. (**C**) Expression levels of cell cycle-related proteins were examined via western blot. (**D**) Relative protein expression levels were normalized to *GAPDH*. * $P < 0.05$

AKT inhibitors blocked the cancer promoting effect of *DDX18* in esophageal cancer

To corroborate our results, KYSE-30 cells overexpressing *DDX18* were treated with the *AKT* inhibitor LY294002 (10 μM). Compared to cells with *DDX18* overexpression alone, those receiving the inhibitor displayed significantly reduced viability (Fig. 5A) and a diminished capacity for colony formation (Fig. 5B). In addition, treatment with the *AKT* inhibitor resulted in a marked decrease in the proportion of S phase and G2/M phase cells, with a corresponding increase in G0/G1 phase cells, relative to the *DDX18* overexpression group (Fig. 5C and D). Furthermore, western blot analysis of cell cycle-related proteins revealed that *Cyclin D1*, *cMyc*, and *CDK4* levels were substantially decreased in the inhibitor-treated, *DDX18*-overexpressing cells (Fig. 5C and D). In contrast, *P21* levels were elevated in these cells compared to those with *DDX18* overexpression only, thereby confirming that *AKT* pathway inhibition suppresses *DDX18*-mediated cell cycle progression.

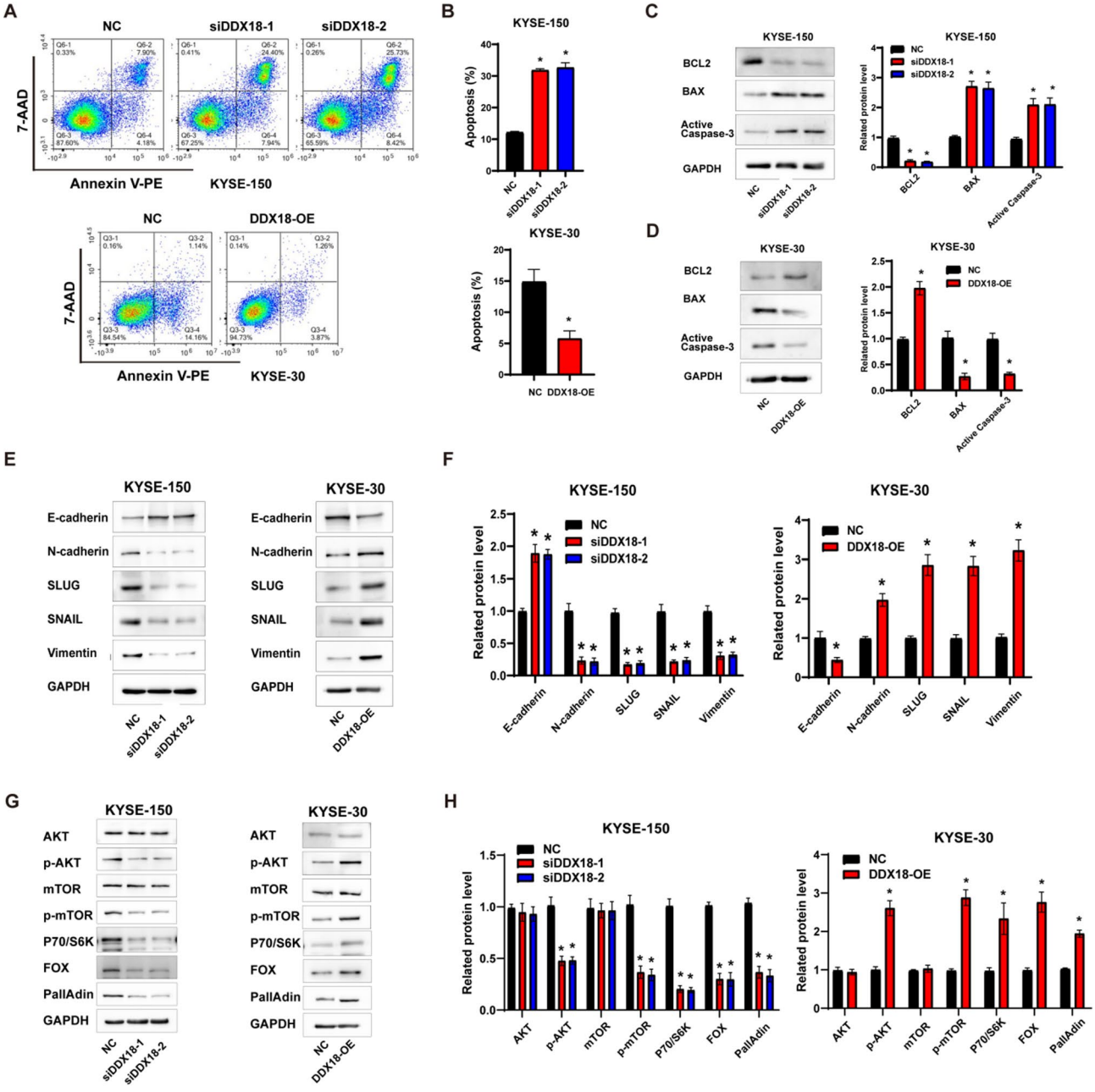

Fig. 4 *DDX18* inhibited apoptosis and induced EMT through *AKT/mTOR* signaling pathway. (**A**) Cell apoptosis was assessed via flow cytometry 24 h post-transfection. (**B**) The percentage of apoptotic cells was quantified using FlowJo software. (**C**, **D**) Expression levels of apoptosis-related proteins were analyzed by western blot in KYSE-150 (**C**) and KYSE-30 (**D**) cells. (**E**) EMT-related protein expression was examined using western blot. (**F**) Relative protein expression levels were normalized to *GAPDH*. (**G**) Western blot analysis of the expression levels of *AKT*, p-*AKT*, *mTOR*, p-*mTOR*, *P70/S6K*, *FOX*, and *Palladin* in KYSE-150 and KYSE-30 cells. (**H**) Relative protein expression levels were normalized to *GAPDH*. * $P < 0.05$

DDX18 promoted KYSE-140 cell proliferation and EMT via activation of the *AKT* signaling pathway

We further substantiated the oncogenic role of *DDX18* in KYSE-140 cells by transfecting them with a *DDX18* overexpression plasmid for 24 h. Following transfection, there was a marked enhancement in cell proliferation (Fig. 6A) and colony formation ability (Fig. 6B). Both Transwell migration and scratch wound healing assays confirmed that *DDX18* upregulation considerably increased cellular migration and invasion (Fig. 6C **and D**). Moreover, *DDX18* overexpression significantly increased the proportions of cells in the S and G2/M phases while reducing those in the G0/G1 phase (Fig. 6E). Western blot analysis demonstrated a significant rise in *Cyclin D1*, *cMyc*, and *CDK4* levels, coupled with a decrease in *p21* in the *DDX18*-overexpressing cells (Fig. 6F). In addition,

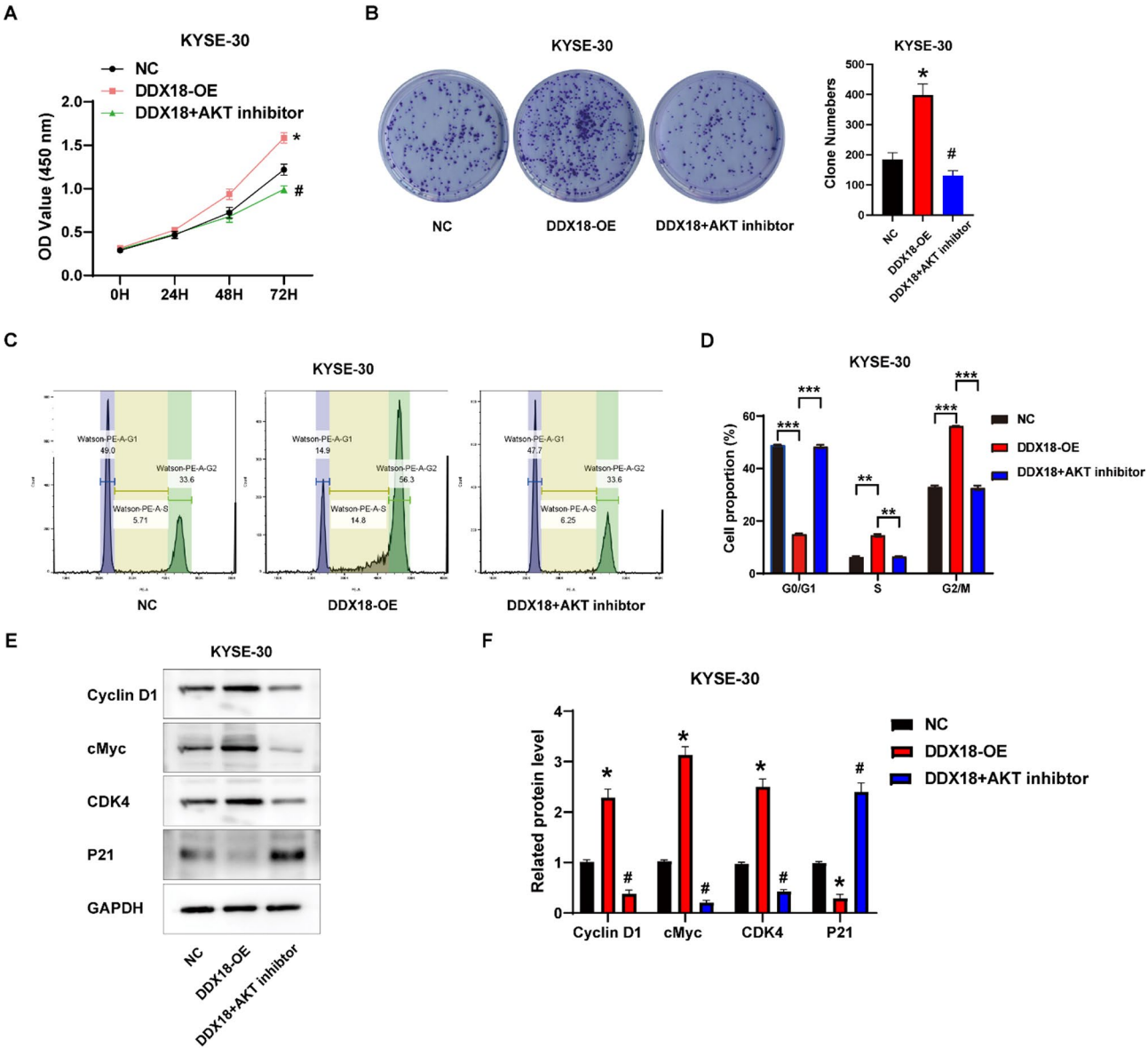

Fig. 5 *AKT* inhibitors blocked the cancer promoting effect of *DDX18* in esophageal cancer. (**A**) KYSE-30 cells overexpressing *DDX18* were treated with the *AKT* inhibitor LY294002 (10 μM) for 24 h, and cell viability was evaluated using the CCK8 assay. (**B**) Images from the colony formation assay were captured 14 days post-transfection. (**C**) Flow cytometry was used to analyze the cell cycle distribution (G0/G1, S, and G2/M phases) in KYSE-30 cells 24 h post-transfection. (**D**) Intergroup differences in cell cycle distribution were compared. (**E**) Expression levels of cell cycle-related proteins were determined by western blot. (**F**) Protein levels were normalized to *GAPDH*. * $P < 0.05$ vs. NC; # $P < 0.05$ vs. *DDX18*-OE; ** $P < 0.01$; *** $P < 0.001$

DDX18 overexpression resulted in a significant reduction in the percentage of apoptotic cells (Fig. 6G), which was accompanied by an increase in pro-apoptotic proteins *BAX* and *active Caspase-3* and a decrease in anti-apoptotic *BCL2* levels (Fig. 6H). Furthermore, overexpression of *DDX18* resulted in the upregulation of epithelial–mesenchymal transition markers including *N-cadherin*, *SLUG*, *SNAIL*, and *Vimentin*, along with a reduction in *E-cadherin* levels (Fig. 6I). Mechanistically, *DDX18* overexpression significantly increased the phosphorylation of *AKT* and *mTOR* and simultaneously upregulated downstream effectors such as *p70/S6K*, *FOX*, and *Palladin* within the *AKT*/*mTOR* signaling cascade (Fig. 6J).

YY1 promoted *DDX18* transcription

To elucidate the molecular mechanism underlying *DDX18* overexpression in esophageal cancer, we performed a bioinformatics analysis using JASPAR (https://jaspar.elixir.no/), which identified *YY1* as a potential transcription factor for *DDX18* (Fig. 7A). To validate this finding, we constructed a *YY1* overexpression plasmid and transfected it into esophageal cancer cells.

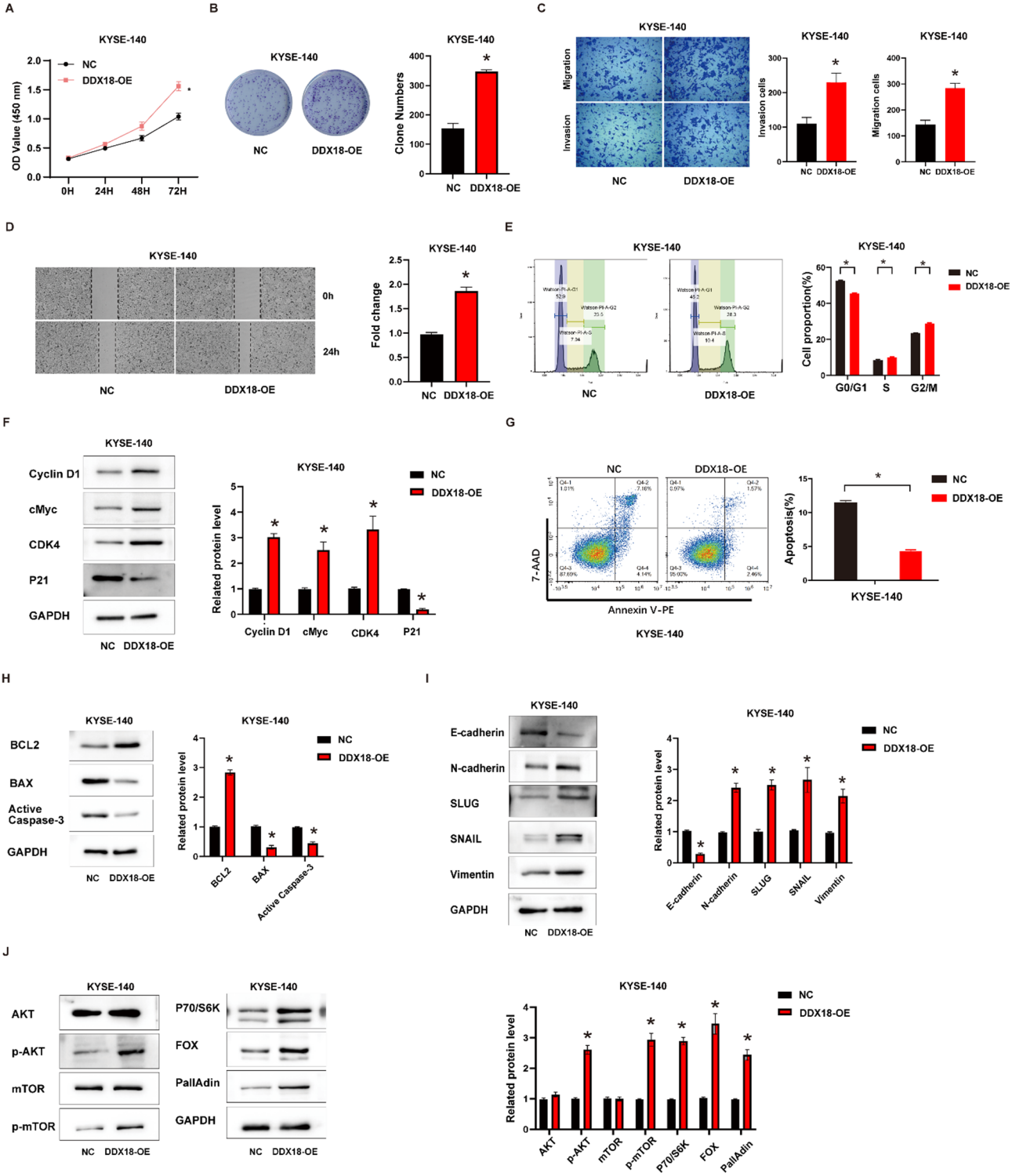

Fig. 6 *DDX18* promoted KYSE-140 cell proliferation and EMT via activation of the *AKT/mTOR* signaling pathway. (**A**) KYSE-140 cells were transfected with a *DDX18* overexpression plasmid for 24 h, then cell proliferation was evaluated using the CCK-8 assay. (**B**) Colony formation images were captured 14 days post-transfection. (**C**) Transwell assays were performed to assess cell migration and invasion, with micrographs taken at 100× magnification. (**D**) Wound healing was imaged at 0 and 24 h at 40× magnification, and the healing area was normalized to that of the control group. (**E**) Cell cycle distribution (G0/G1, S, and G2/M phases) was analyzed by flow cytometry. (**F**) Cell cycle-related protein expression was determined using western blot. (**G**) Apoptosis was assessed by flow cytometry 24 h post-transfection. (**H**) Apoptosis-related proteins were measured by western blot. (**I**) EMT-related proteins were detected via western blot. (**J**) *AKT/mTOR* pathway-related proteins were analyzed by western blot, with protein levels normalized to *GAPDH*. * $P < 0.05$

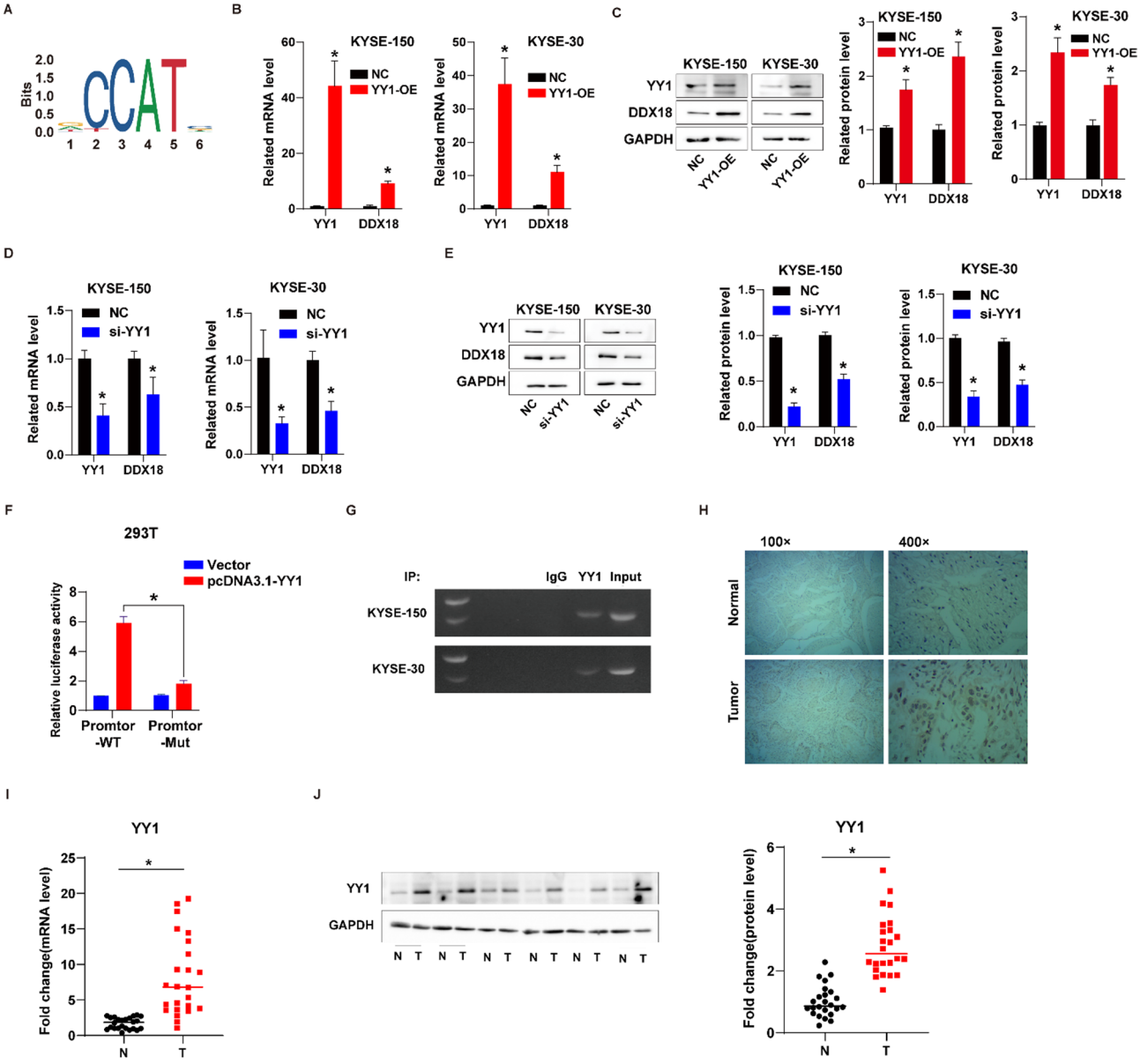

Fig. 7 Transcription factor *YY1* promoted *DDX18* transcription in esophageal cancer cells. (**A**) Bioinformatics analysis predicted *YY1* binding sites within the *DDX18* promoter region (https://jaspar.elixir.no/). (**B**) KYSE-150 and KYSE-30 cells were transfected with a *YY1* overexpression plasmid, and qPCR was used to quantify the mRNA levels of *YY1* and *DDX18*. (**C**) Western blot analysis was performed to assess *YY1* and *DDX18* protein expression in control and *YY1*-overexpressing cells. (**D**) KYSE-150 and KYSE-30 cells were transfected with *YY1* siRNA, followed by qPCR to measure *YY1* and *DDX18* mRNA levels. (**E**) Western blotting evaluated *YY1* and *DDX18* protein levels in control and *YY1*-knockdown cells. (**F**) 293T cells were co-transfected with luciferase vectors containing either the wild-type or mutant *DDX18* promoter and the *YY1* plasmid, after which luciferase activity was quantified. (**G**) ChIP assay was performed to verify the binding of *YY1* to the *DDX18* promoter. (**H**) *YY1* expression was detected by immunohistochemistry in a tissue array consisting of 45 esophageal cancer tissues and 45 adjacent non-tumor tissues. (**I**) qPCR analysis was used to evaluate *YY1* mRNA levels in 24 paired esophageal cancer and adjacent non-tumor tissues. (**J**) Western blot analysis determined *YY1* protein expression in 24 paired esophageal cancer and adjacent non-tumor tissues, with *GAPDH* serving as the loading control. * $P < 0.05$

qPCR analysis revealed that *YY1* overexpression markedly increased *DDX18* mRNA levels in both KYSE-150 and KYSE-30 cells (Fig. 7B), a result that was corroborated at the protein level by western blotting (Fig. 7C). In contrast, *YY1* knockdown significantly reduced both the mRNA and protein expression of *DDX18* (Fig. 7D and E).

Furthermore, a dual luciferase assay conducted in 293T cells confirmed the binding of *YY1* to the *DDX18* promoter: co-transfection of *YY1* with the wild-type *DDX18* promoter resulted in a significant enhancement in luciferase activity compared with co-transfection with a mutant promoter (Fig. 7F). Chromatin immunoprecipitation

Table 3 *YY1* expression in EC compared with para-carcinoma tissue

Group	*n*	YY1 expression		*P*
		Low (n%)	High (n%)	
EC	45	20 (44.4)	25 (55.6)	0.010*
Para-carcinoma	45	33 (73.3)	12 (26.7)	

* $P < 0.05$

Table 4 *YY1* expression associated with the clinicopathological parameters in esophageal cancer

Clinicopathological parameters	*n*	YY1 Low (*n*%)	YY1 High (*n*%)	*P*
Gender				
Male	41	20 (48.8)	21 (51.2)	0.178
Female	4	0 (0.0)	4 (100.0)	
Age (years)				
≤65	25	11 (44.0)	14 (56.0)	0.814
>65	20	9 (45.0)	11 (55.0)	
Pathological grading				
I-II	33	20 (60.6)	13 (39.4)	0.001**
III	12	0 (0.0)	12 (100.0)	

** $P < 0.01$

(ChIP) assays further demonstrated a robust interaction between *YY1* and the *DDX18* promoter in both KYSE-150 and KYSE-30 cells (Fig. 7G). Taken together, these findings indicate that *YY1* directly promotes the transcription of *DDX18* in esophageal cancer cells.

YY1 was upregulated in esophageal cancer

Immunohistochemical analysis of a tissue array containing specimens from 45 esophageal cancer patients (Fig. 7H) revealed that *YY1* was significantly upregulated in tumor tissues (25 out of 45, 55.6%) compared with adjacent non-tumor tissues (12 out of 45, 26.7%) (Table 3). Moreover, *YY1* expression was significantly higher in patients with pathological grade III tumors (12 out of 12, 100.0%) than in those with grade I–II (13 out of 33, 39.4%) (Table 4). qPCR and western blot analyses of 24 paired clinical samples further confirmed that *YY1* expression was elevated in tumor tissues relative to para-carcinoma tissues (Fig. 7I and J).

YY1 reversed the inhibition effect of *DDX18* knockdown on esophageal cancer cells

Subsequently, A rescue assay was conducted to validate the interaction between *YY1* and *DDX18* and their functional effects on esophageal cancer cells. *YY1* overexpression plasmid and *DDX18* siRNAs were co-transfected into KYSE-150 and TE-1 cells. As shown in Fig. 8A, cell viability was significantly increased in the co-transfected group compared with cells transfected with *DDX18* siRNAs alone. Similarly, colony formation assays demonstrated a significant increase in colony number in co-transfected cells (Fig. 8B and C).

YY1 also counteracted the inhibitory effects of *DDX18* knockdown on cell migration and invasion. Transwell assays confirmed that *YY1* overexpression restored the migration and invasion capacity reduced by *DDX18* knockdown in KYSE-150 and TE-1 cells (Fig. 8D-G). Consistently, the wound healing assay showed that *YY1* overexpression increased the wound closure area in co-transfected cells compared with *DDX18* knockdown cells (Fig. 8H and I).

Flow cytometry analysis revealed an increased proportion of G2/M phase cells in the co-transfected group compared with the *DDX18* knockdown group in both KYSE-150 and TE-1 cells (Fig. 9A and B). Additionally, western blot analysis demonstrated that *Cyclin D1*, *cMyc*, and *CDK4* expression was upregulated in co-transfected cells compared to *DDX18* knockdown cells, whereas *P21* levels exhibited the opposite trend (Fig. 9C and D).

Furthermore, the increase in apoptosis induced by *DDX18* knockdown was suppressed by *YY1* overexpression in both KYSE-150 and TE-1 cells (Fig. 10A and B). *YY1* overexpression also reversed the abnormal expression of apoptosis-related proteins caused by *DDX18* silencing (Fig. 10C and D). Collectively, these findings confirm that *YY1* reverses the effect of *DDX18* knockdown in esophageal cancer cells.

YY1 rescued the effects of *DDX18* on EMT and *AKT/mTOR* pathway

Western blot analysis revealed that the upregulation of the epithelial marker *E-cadherin* induced by *DDX18* knockdown was reversed by *YY1* overexpression. In parallel, mesenchymal markers (*N-cadherin*, *SLUG*, *SNAIL*, and *Vimentin*) were increased in the co-transfected cells compared with those with *DDX18* knockdown alone (Fig. 10E and F). Additionally, *YY1* overexpression restored the phosphorylation levels of *AKT* and *mTOR* and elevated the expression of downstream molecules *P70/S6K*, *FOX*, and *Palladin* in *DDX18* knockdown cells (Fig. 10G and H). These results indicate that *YY1* overexpression reverses the regulation of *DDX18* knockdown on EMT and *AKT/mTOR* pathway in esophageal cancer.

DDX18 promoted esophageal cancer growth in vivo

In a xenograft mouse model, *DDX18* knockdown significantly reduced tumor volume. Notably, the tumor growth inhibition induced by *DDX18* siRNAs was reversed upon co-expression of *YY1* (Fig. 11A). Immunohistochemical analysis confirmed a strong decrease in *DDX18* expression in the knockdown group, accompanied by a significant reduction in *KI67* staining (Fig. 11B and C). Both immunohistochemical and western blot analyses corroborated that *YY1* overexpression markedly increased *DDX18* expression. Our results indicate that *DDX18* assists esophageal cancer growth in vivo.

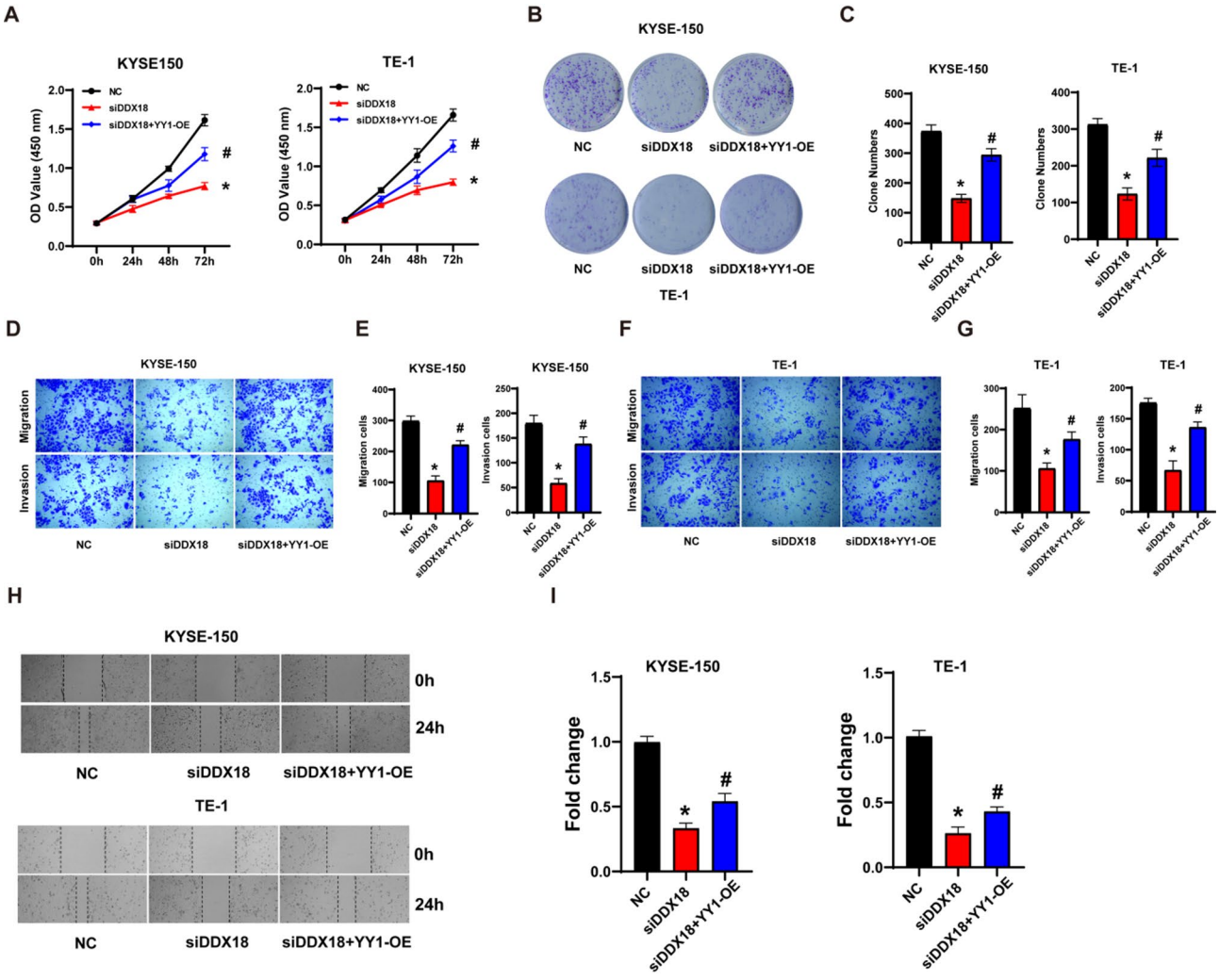

Fig. 8 *YY1* overexpression reversed the inhibition of proliferation, migration, and invasion induced by *DDX18* knockdown. (**A**) KYSE-150 and TE-1 cells were co-transfected with *YY1* overexpression plasmid and *DDX18* siRNA. Cell viability was assessed using the CCK8 assay. (**B**) Colony formation assay images were captured 14 days post-transfection. (**C**) Colony count was performed for each group. (**D**, **E**) Migration and invasion of KYSE-150 cells were assessed using Transwell assays. (**F**, **G**) Migration and invasion of TE-1 cells were also assessed via Transwell assays. Micrographs were taken at 100× magnification. (**H**) Wound healing was imaged at 0 and 24 h at 40× magnification. (**I**) The healing area was normalized to the control group. * $P < 0.05$ vs. NC, # $P < 0.05$ vs. si*DDX18*

Discussion

This study identifies *DDX18* as an oncogene in esophageal cancer. Tissue microarrays and clinical samples confirmed that *DDX18* is highly expressed in esophageal cancer and is strongly associated with higher pathological grades, suggesting its involvement in tumor progression.

Previous studies have indicated that *DDX18* contributes to tumorigenesis by facilitating immune evasion and promoting tumor cell proliferation [10, 11]. Our findings further demonstrate that knockdown of *DDX18* suppresses the proliferation, migration, and invasion of esophageal cancer cells while enhancing apoptosis, whereas its overexpression produces the opposite effects. Notably, *DDX18* was also found to drive epithelial-mesenchymal transition (EMT) in esophageal cancer cells, as evidenced by the regulation of mesenchymal and epithelial markers. Since aberrant EMT is closely linked to tumor invasion and metastasis [15, 16], these findings suggest that *DDX18* plays a critical role in esophageal cancer progression.

The *AKT*/*mTOR* signaling pathway is a key regulatory axis in cell proliferation, cell cycle progression, and migration [17, 18]. This pathway is highly relevant to tumorigenesis and represents an important therapeutic target [19–21]. Our study confirmed that in esophageal cancer cells, knockdown of *DDX18* reduces the phosphorylation of *AKT* and *mTOR*, whereas its overexpression enhances activation of the *AKT*/*mTOR* pathway. Although *DDX18* has been reported to activate

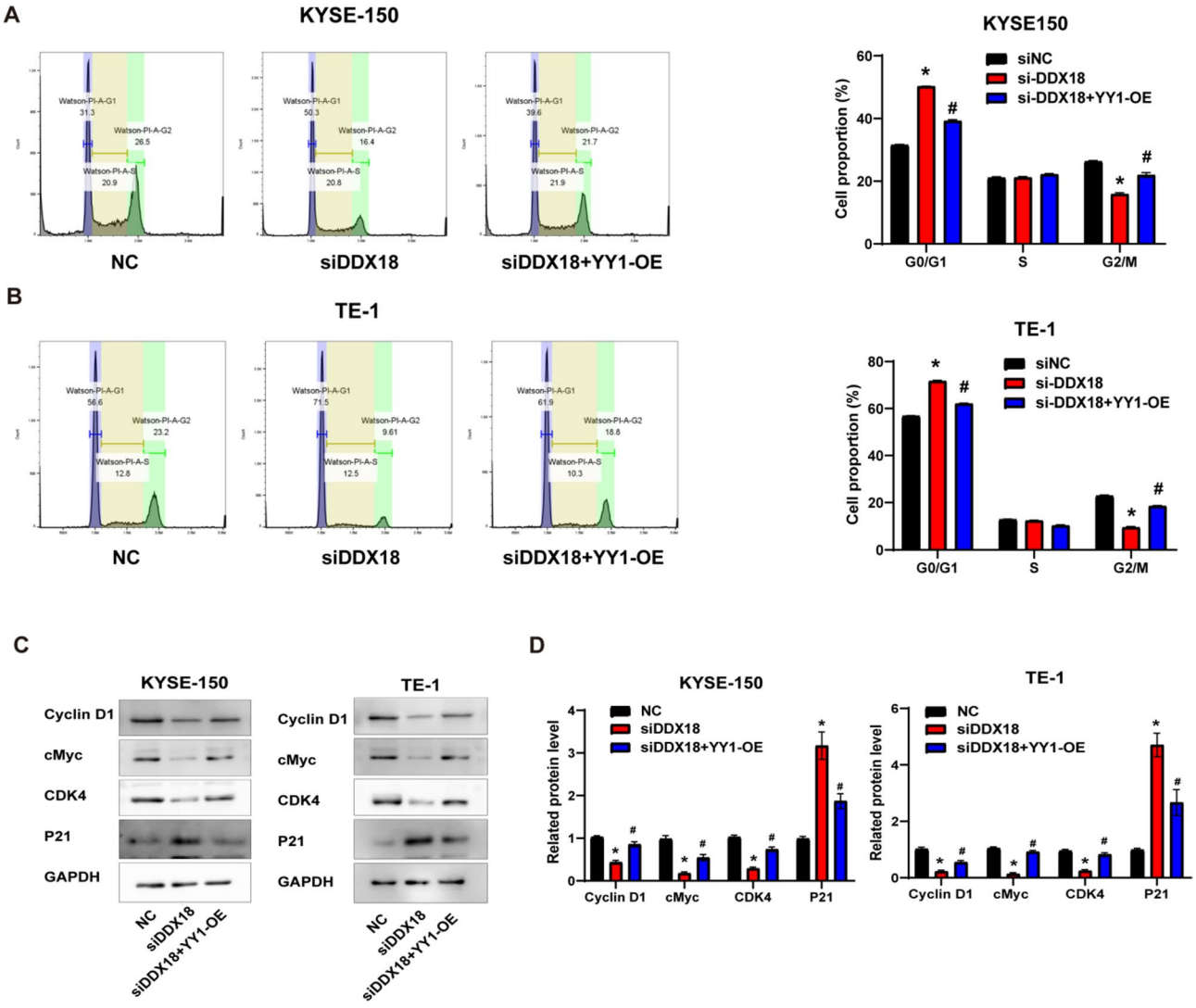

Fig. 9 *YY1* overexpression reversed the effect of *DDX18* on cell cycle. KYSE-150 (**A**) and TE-1 (**B**) cells were collected 24 h after transfection, and cell cycle distribution (G0/G1, S, G2/M phases) was analyzed using flow cytometry. (**C**) Cell cycle-related proteins were assessed by western blot analysis. (**D**) Protein expression levels were normalized to *GAPDH*. * $P < 0.05$ vs. NC; # $P < 0.05$ vs. si*DDX18*

AKT signaling in gastric cancer, its precise mechanism remains unclear [11].

Through bioinformatics analysis, we identified *YY1* as a transcriptional regulator of *DDX18*. *YY1* is a zinc finger transcription factor belonging to the GLI-Kruppel family and plays a critical role in various biological processes [22]. Numerous studies have highlighted its significant involvement in esophageal cancer progression [23–25]. Clinically, *YY1* is aberrantly upregulated in lymph node metastases and advanced esophageal cancer tissues [26], and its overexpression promotes tumor growth, invasion, and overall malignancy [27–29]. Furthermore, *YY1* has been linked to immune cell infiltration and may contribute to tumor immune evasion [30]. It is also highly expressed in radiation-resistant tissues and is associated with shorter overall survival in patients with esophageal cancer [31], while its knockdown has been shown to enhance radiosensitivity both in vitro and in vivo [31, 32]. Notably, this study is the first to demonstrate that *YY1* directly regulates *DDX18* transcription. Luciferase assays confirmed that *YY1* binds to the *DDX18* promoter, resulting in increased *DDX18* expression, whereas *YY1* knockdown leads to a reduction in *DDX18* levels.

Finally, in vivo experiments validated the oncogenic role of *DDX18* and its regulation by *YY1*. *DDX18* knockdown significantly suppressed tumor growth, but this effect was counteracted by *YY1* overexpression. These results highlight *DDX18* as a promising therapeutic target for esophageal cancer, warranting further clinical translational research.

In conclusion, *DDX18* is highly expressed in esophageal cancer and promotes tumor cell growth and EMT via

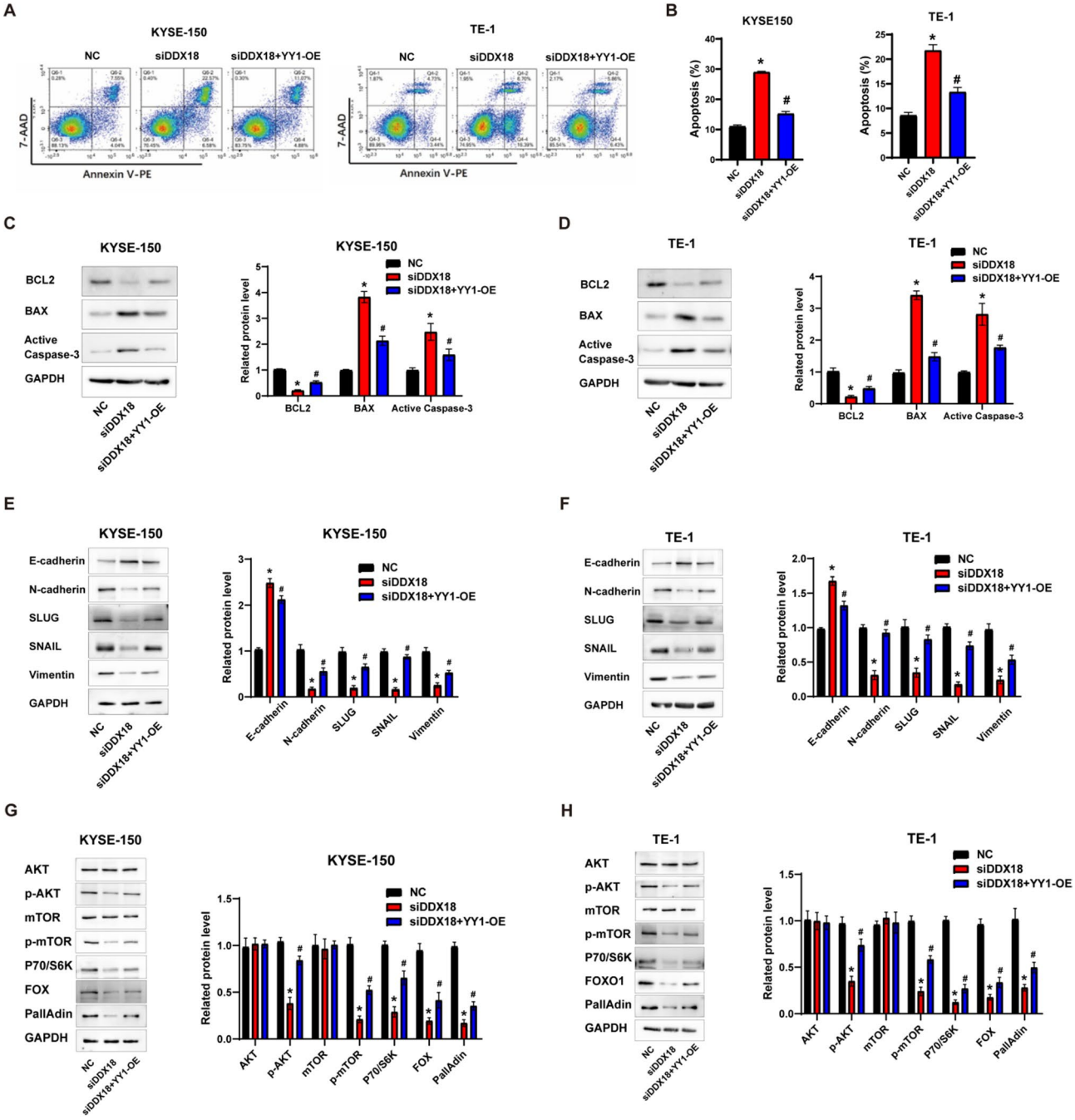

Fig. 10 *YY1* rescued the effects of *DDX18* on apoptosis and EMT. (**A**) Apoptosis was analyzed by flow cytometry 24 h post-transfection in KYSE-150 and TE-1 cells. (**B**) The percentage of apoptotic cells was quantified in KYSE-150 and TE-1 cells using FlowJo software. (**C**, **D**) The expression levels of apoptosis-related proteins were assessed by western blot in KYSE-150 (**C**) and TE-1 (**D**) cells. (**E**, **F**) EMT-related proteins were analyzed via western blot in KYSE-150(**E**) and TE-1(**F**) cells. (**G**, **H**) Western blot analysis of the expression levels of *AKT*, p-*AKT*, *mTOR*, p-*mTOR*, *P70/S6K*, *FOX*, and *Palladin* in KYSE-150(**G**) and TE-1(**H**) cells. *GAPDH* was used as a loading control. * $P < 0.05$ vs. NC; # $P < 0.05$ vs. si*DDX18*

the *AKT*/*mTOR* signaling pathway. *YY1* induces *DDX18* transcription by directly binding to its promoter. This study expands the regulatory network underlying esophageal cancer progression and provides novel insights for potential therapeutic strategies.

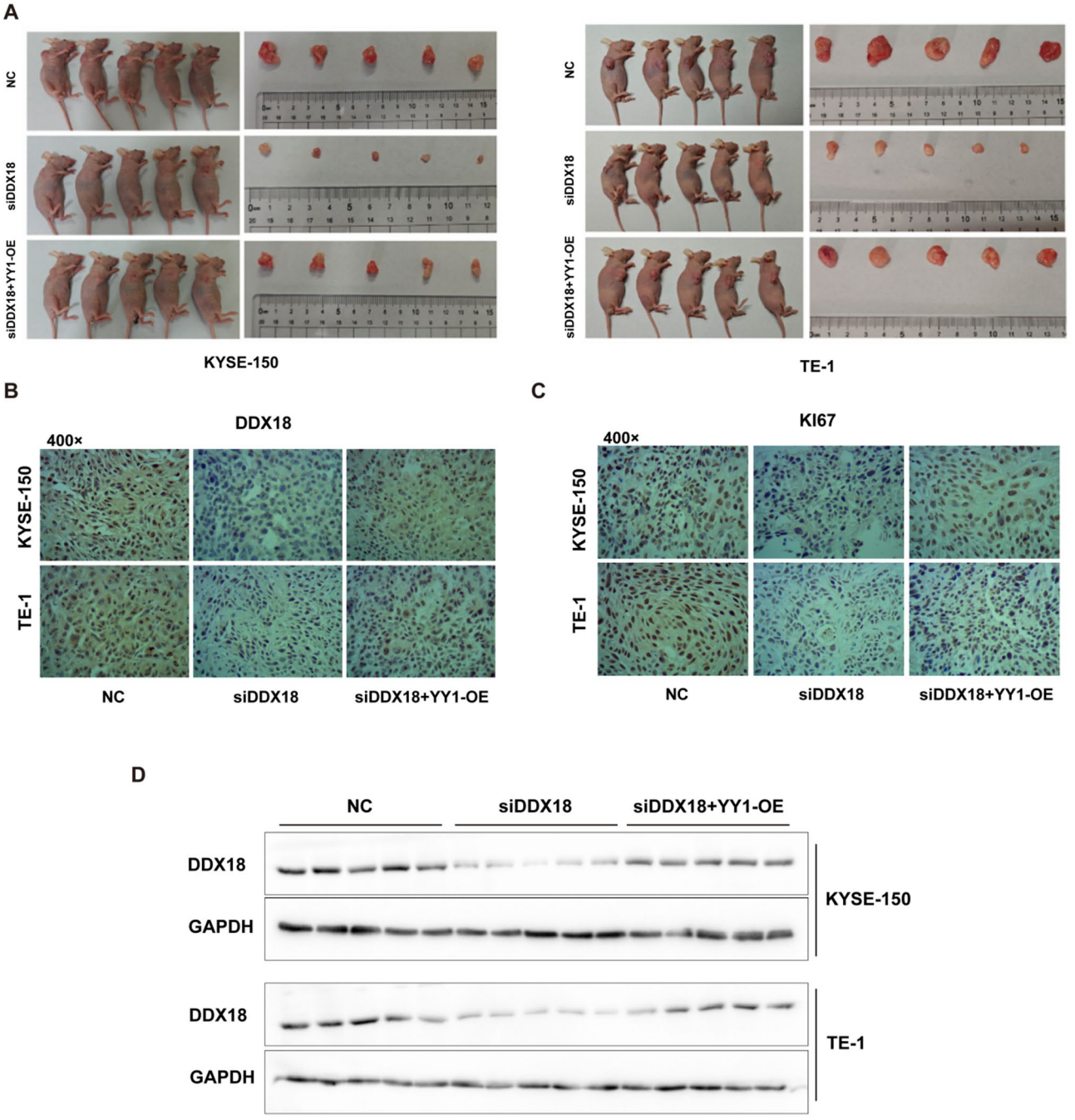

Fig. 11 *DDX18* promoted the growth of esophageal cancer in vivo. (**A**) Female BALB/C mice ($n=5$) were injected with 1×10^6 KYSE-150 or TE-1 cells. Tumor volume was measured 24 days post-injection. (**B**) Immunohistochemical analysis was conducted to assess *DDX18* levels in tumor tissue from the mice. Micrographs were captured at 400× magnification. (**C**) *KI67* expression was evaluated by immunohistochemical staining. Micrographs were taken at 400× magnification. (**D**) *DDX18* expression was further confirmed through western blot analysis

Supplementary Information

The online version contains supplementary material available at https://doi.org/10.1186/s12967-025-06555-7.

Supplementary Material 1

Acknowledgements
Not applicable.

Author contributions
Xiaochao Ma and Yulu He do experiments and write manuscript. Yue Yang, Tianyu Lu and Ze Tang participates in the experiment. Youbin Cui and Rui Wang revise the manuscript.

Funding
This work was supported by Jilin Provincial Department of Science and Technology Project (20130604050TC).

Data availability
The data supporting the conclusions of this paper are included within the manuscript.

Declarations

Ethics approval and consent to participate
This research study was approved by the Institutional Review Board of The First Hospital of Jilin University.

Consent for publication
Not applicable.

Competing interests
The authors declare that they have no competing interests.

Received: 11 December 2024 / Accepted: 30 April 2025
Published online: 20 May 2025

References

1. Bray F, Laversanne M. Global cancer statistics 2022: GLOBOCAN estimates of incidence and mortality worldwide for 36 cancers in 185 countries [J]. Cancer J Clin. 2024;74(3):229–63.
2. Eisner D C. Esophageal cancer: treatment advances and need for screening [J]. Jaapa. 2024;37(4):19–24.
3. Domper Arnal M J, Ferrández Arenas, Á, Lanas Arbeloa Á. Esophageal cancer: risk factors, screening and endoscopic treatment in Western and Eastern countries [J]. World J Gastroenterol. 2015;21(26):7933–43.
4. Sakanaka K. Treatment strategy for early-stage esophageal cancer [J]. Japanese J Radiol. 2024;42(7):677–84.
5. Deboever N, Jones C M, Yamashita K, et al. Advances in diagnosis and management of cancer of the esophagus [J]. BMJ. 2024;385:e074962.
6. Zhang H, Wu Z, Lu J Y, et al. DEAD-Box helicase 18 counteracts PRC2 to safeguard ribosomal DNA in pluripotency regulation [J]. Cell Rep. 2020;30(1):81–e977.
7. Schütz P, Karlberg T, Van Den Berg S et al. Comparative structural analysis of human DEAD-box RNA helicases [J]. PLoS ONE, 2010, 5(9).
8. Jin H, Zhou L, Ge X, et al. Cellular DEAD-box RNA helicase 18 (*DDX18*) promotes the PRRSV replication via interaction with virus nsp2 and nsp10 [J]. Virus Res. 2017;238:204–12.
9. Payne E M, Bolli N, Rhodes J, et al. *Ddx18* is essential for cell-cycle progression in zebrafish hematopoietic cells and is mutated in human AML [J]. Blood. 2011;118(4):903–15.
10. Dong G, Wang Q, Wen M, et al. *DDX18* drives tumor immune escape through transcription-activated STAT1 expression in pancreatic cancer [J]. Oncogene. 2023;42(40):3000–14.
11. Zhang Y, Yu F, Ni B, et al. The RNA-Binding protein *DDX18* promotes gastric Cancer by affecting the maturation of MicroRNA-21 [J]. Front Oncol. 2020;10:598238.
12. Redmond A M, Byrne C, Bane F T, et al. Genomic interaction between ER and HMGB2 identifies *DDX18* as a novel driver of endocrine resistance in breast cancer cells [J]. Oncogene. 2015;34(29):3871–80.
13. Chen N, Zhang G, Fu J, et al. Identification of key modules and hub genes involved in esophageal squamous cell carcinoma tumorigenesis using WCGNA [J]. Cancer Control: J Moffitt Cancer Cent. 2020;27(1):1073274820978817.
14. Rauluseviciute I, Riudavets-Puig R, Blanc-Mathieu R et al. Jaspar. 2024: 20th anniversary of the open-access database of transcription factor binding profiles [J]. Nucleic Acids Res. 2024;52(D1):D174-d82.
15. Chen L, Zhu S, Liu T, et al. Aberrant epithelial cell interaction promotes esophageal squamous-cell carcinoma development and progression [J]. Signal Transduct Target Ther. 2023;8(1):453.
16. Huang C M, Huang C S, Hsu T N et al. Disruption of Cancer metabolic SREBP1/miR-142-5p suppresses Epithelial-Mesenchymal transition and stemness in esophageal carcinoma [J]. Cells, 2019, 9(1).
17. Chen Y, Guan W, Wang ML et al. PI3K-*AKT*/*mTOR* signaling in psychiatric disorders: A valuable target to stimulate or suppress?? [J]. Int J Neuropsychopharmacol, 2024, 27(2).
18. Xu F, Na L, Li Y, et al. Roles of the PI3K/*AKT*/*mTOR* signalling pathways in neurodegenerative diseases and tumours [J]. Cell Biosci. 2020;10(1):54.
19. Peng Y, Wang Y, Zhou C, et al. PI3K/*Akt*/*mTOR* pathway and its role in Cancer therapeutics: are we making headway?? [J]. Front Oncol. 2022;12:819128.
20. Yu L, Wei J. Attacking the PI3K/*Akt*/*mTOR* signaling pathway for targeted therapeutic treatment in human cancer [J]. Semin Cancer Biol. 2022;85:69–94.
21. Luo Q, Du R, Liu W, et al. PI3K/*Akt*/*mTOR* signaling pathway: role in esophageal squamous cell carcinoma, regulatory mechanisms and opportunities for targeted therapy [J]. Front Oncol. 2022;12:852383.
22. Lee Js, See R H, Galvin K M, et al. Functional interactions between *YY1* and adenovirus E1A [J]. Nucleic Acids Res. 1995;23(6):925–31.
23. Luo J, Zhou X, Ge X, et al. Upregulation of Ying Yang 1 (*YY1*) suppresses esophageal squamous cell carcinoma development through Heme oxygenase-1 [J]. Cancer Sci. 2013;104(11):1544–51.
24. Zhong B, Shingyoji M. A p53-stabilizing agent, CP-31398, induces *p21* expression with increased G2/M phase through the *YY1* transcription factor in esophageal carcinoma defective of the p53 pathway [J]. Am J cancer Res. 2019;9(1):79–93.
25. Nie J, Ge X, Geng Y, et al. miR-34a inhibits the migration and invasion of esophageal squamous cell carcinoma by targeting Yin Yang-1 [J]. Oncol Rep. 2015;34(1):311–7.
26. Luo J, Jiang X. Expression of *YY1* correlates with progression and metastasis in esophageal squamous cell carcinomas [J]. OncoTargets Therapy. 2014;7:1753–9.
27. Cheng J, Yang Q, Han X, et al. Yin Yang 1-stimulated long noncoding RNA bladder cancer-associated transcript 1 upregulation facilitates esophageal carcinoma progression via the microRNA-5590-3p/programmed cell death-ligand 1 pathway [J]. Bioengineered. 2022;13(4):10244–57.
28. Deng W, Fan W, Li P, et al. microRNA-497-mediated Smurf2/*YY1*/HIF2α axis in tumor growth and metastasis of esophageal squamous cell carcinoma [J]. J Biochem Mol Toxicol. 2022;36(11):e23182.
29. Li Y, Li T, Yang Y, et al. *YY1*-induced upregulation of *FOX*P4-AS1 and *FOX*P4 promote the proliferation of esophageal squamous cell carcinoma cells [J]. Cell Biol Int. 2020;44(7):1447–57.
30. Luo C, Chen X, Bai Y et al. Upregulation of Yin-Yang-1 Associates with Proliferation and Glutamine Metabolism in Esophageal Carcinoma [J]. International journal of genomics. 2022;2022:9305081.
31. Zheng C, Li Z, Zhao C, et al. *YY1* modulates the radiosensitivity of esophageal squamous cell carcinoma through KIF3B-mediated Hippo signaling pathway [J]. Volume 14. Cell death & disease; 2023. p. 806. 12.
32. Zhao M, Lu T, Bi G, et al. PLK1 regulating chemoradiotherapy sensitivity of esophageal squamous cell carcinoma through Pentose phosphate pathway/ferroptosis [J]. Volume 168. Biomedicine & pharmacotherapy = Biomedecine & pharmacotherapie; 2023. p. 115711.

Publisher's note